

A Refinement of the Analytic Function Expansion Nodal Method with Interface Flux Moments

Sweng Woong Woo and Nam Zin Cho

Korea Advanced Institute of Science and Technology
Department of Nuclear Engineering
373-1 Kusong-dong, Yusong-gu
Taejon, Korea 305-701

Jae Man Noh

Korea Atomic Energy Research Institute
150 Dukjin-dong, Yusong-gu
Taejon, Korea 305-353

Abstract

A refinement of the AFEN method has been performed by increasing the number of flux expansion terms in the manner that the original basis functions are combined with the transverse-direction linear functions. In this manner, the added terms can be kept to still satisfy the diffusion equation. The additional constraints required are provided by the interface flux moments defined as the weighted-average fluxes at the interface.

The refined AFEN method was tested against the OECD-L336 benchmark problem. The results show that the method improves the accuracy in predicting the flux distribution and that it can replace the corner-point fluxes with the interface moments without accuracy degradation. Excluding the corner-point flux increases the flexibility in implementing this method into the existing codes that do not have the corner-point flux scheme and may make it fit better for the non-linear scheme based on two-node problems.

I. Introduction

The Analytic Function Expansion Nodal (AFEN) method has been developed and successfully applied to the analyses of the reactor cores in both rectangular and hexagonal geometries.[1-3] The success of the AFEN method is attributed to its accuracy in solving the nodal diffusion equations and its flexibility in treating various geometries appearing in the usual reactor analysis. The main feature of the AFEN method is that it expands the solution of the multidimensional diffusion equation in each node into the non-separable analytic basis functions which satisfies the diffusion equation everywhere in the node. Furthermore, it applies relatively tight constraints constraining the core-wise flux distribution, such as the nodal neutron balance conditions, the interface flux and current continuity conditions, the corner-point flux continuity conditions, and the corner-point leakage balance conditions. Expanding the intranodal flux into the functions satisfying the diffusion equation locally and

applying the tight constraints guarantee the accuracy of the AFEN method.

In this paper, a refinement of the AFEN method is proposed to improve accuracy further so that it should satisfy the potential demand requiring very high accuracy in both the nodal calculation and the pin-flux reconstruction calculation and to widen the spectrum of its implementations to various existing nodal codes. This refinement is performed by adding basis functions to the original flux expansion. The added functions are the products of the trigonometric functions (or the hyperbolic trigonometric functions) in a direction and possible combinations of the linear functions in the transverse directions to the direction of the trigonometric function (e.g., $y \sin(kx)$, $z \sin(kx)$, and $yz \sin(kx)$). They also satisfy the diffusion equation at any point in the node. The additional constraints required by the added terms are the continuity conditions of the flux moments and the current moments at the interfaces. These interface moments are defined by the interface-average fluxes weighted by the odd functions in the parallel directions to the interface (e.g., averages of $y \phi(x,y,z)$, $z \phi(x,y,z)$, and $yz \phi(x,y,z)$ over y and z at an interface perpendicular to the x axis). A simple choice of the weighting functions is a step or a linear function with alternating sign about the center of the interface. If we choose the step function as a weighting function of the interface flux moment, the method is equivalent to the one that applies the flux and current continuity conditions at each quadrant of an interface. Since the refined flux expansion also satisfies the diffusion equation and the additional constraints are applied, the salient feature of the original AFEN method is even more enforced in the refined method.

The original AFEN method expands the homogeneous flux in a node in three-dimensional rectangular geometry into 19 analytic basis function terms whose coefficients are determined by 19 nodal unknowns consisting of one node-average flux, six interface fluxes, and twelve edge fluxes. We may increase this number of the nodal unknowns up to 49, noting that three flux moments per interface and one per edge can be included in the nodal unknowns in the refined method. (The edge moment here is defined by the average of the flux weighted by a linear or a step function along the edge-line direction.) This may be unnecessarily too detailed for the homogenous flux expansion even for the rod nodes or the plutonium-bearing nodes that show steep flux gradients. Therefore, it may be sufficient enough to take the node average flux, the interface fluxes, and the interface moments only as the nodal unknowns in the refined method. Since the method uses 25 expansion terms even in this case compared to 19 terms in the original AFEN method, better accuracy is expected. Excluding the edge quantities may reduce the efforts required in implementing this method into the existing nodal codes that use only the node-average flux and the interface quantities as unknowns such as interface fluxes, currents, or partial currents. This can also eliminate the difficulties involved in the non-linear iterative scheme of the original AFEN method induced by the edge fluxes. This version of the AFEN method seems to fit better for the non-linear scheme based on two-node problems that are solved for the interface quantities of the two nodes and is expected better performance.

II. Methodology

II.A. Intranodal Flux Expansion

To expand the intranodal homogeneous flux of a three-dimensional node into analytic basis functions, consider the three-dimensional multi-group diffusion equation in the node:

$$-\mathbf{D}^n \nabla^2 \hat{\mathbf{f}}^n(x, y, z) + \mathbf{S}^n \hat{\mathbf{f}}^n(x, y, z) = \frac{1}{k_{\text{eff}}} \mathbf{nS}_f^n \hat{\mathbf{f}}^n(x, y, z), \quad (1)$$

where the hat (^) on the neutron flux denotes the homogeneous flux which is allowed to be discontinuous across the boundary of the node according to the equivalence theory. [4,5]

In contrast to the most advanced nodal methods that solve the transverse-integrated equivalent one-dimensional diffusion equations, AFEN solves directly this two-dimensional diffusion equation. The general solution of the diffusion equation (1) in the Cartesian coordinate is given in matrix function form by

$$\hat{\mathbf{f}}^n(x, y, z) = \int_{\Gamma} \left[\sinh(\sqrt{\mathbf{L}^n} \mathbf{t}_1 \cdot \mathbf{r}) \{ \mathbf{A}'_0(\mathbf{t}_1) + \mathbf{t}_2 \cdot \mathbf{r} \mathbf{A}'_1(\mathbf{t}_1) + \mathbf{t}_3 \cdot \mathbf{r} \mathbf{A}'_2(\mathbf{t}_1) + (\mathbf{t}_2 \cdot \mathbf{r})(\mathbf{t}_3 \cdot \mathbf{r}) \mathbf{A}'_3(\mathbf{t}_1) \} \right. \\ \left. + \cosh(\sqrt{\mathbf{L}^n} \mathbf{t}_1 \cdot \mathbf{r}) \{ \mathbf{B}'_0(\mathbf{t}_1) + \mathbf{t}_2 \cdot \mathbf{r} \mathbf{B}'_1(\mathbf{t}_1) + \mathbf{t}_3 \cdot \mathbf{r} \mathbf{B}'_2(\mathbf{t}_1) + (\mathbf{t}_2 \cdot \mathbf{r})(\mathbf{t}_3 \cdot \mathbf{r}) \mathbf{B}'_3(\mathbf{t}_1) \} \right] d\mathbf{t}_1, \quad (2)$$

where

$$\mathbf{L}^n = (\mathbf{D}^n)^{-1} \left(\mathbf{S}^n - \frac{1}{k_{\text{eff}}} \mathbf{nS}_f^n \right), \quad (3)$$

$\mathbf{r} = x\mathbf{i} + y\mathbf{j} + z\mathbf{k}$ for unit vectors \mathbf{i} , \mathbf{j} , and \mathbf{k} in x, y, and z directions, respectively,

\mathbf{t}_i on Γ , $\mathbf{t}_i = \alpha_i \mathbf{i} + \beta_i \mathbf{j} + \gamma_i \mathbf{k}$, and $\alpha_i^2 + \beta_i^2 + \gamma_i^2 = 1$ for complex $\alpha_i, \beta_i, \gamma_i$,

$\mathbf{t}_1 \cdot \mathbf{t}_2 = 0$, $\mathbf{t}_2 \cdot \mathbf{t}_3 = 0$, $\mathbf{t}_3 \cdot \mathbf{t}_1 = 0$ for $\mathbf{t}_1, \mathbf{t}_2, \mathbf{t}_3$.

Evaluation of matrix functions in this equation is described in Ref.[6].

This equation shows that, for an arbitrary choice of $\mathbf{t}_1 = (\alpha_1, \beta_1, \gamma_1)$ in the complex domain, not only the sine and cosine hyperbolic functions of $\mathbf{t}_1 \cdot \mathbf{r}$, but also their products multiplied by the linear functions $\mathbf{t}_2 \cdot \mathbf{r}$, $\mathbf{t}_3 \cdot \mathbf{r}$, and their combination $(\mathbf{t}_2 \cdot \mathbf{r})(\mathbf{t}_3 \cdot \mathbf{r})$ are the solutions of the diffusion equation (1) with \mathbf{t}_2 and \mathbf{t}_3 satisfying $\mathbf{t}_2 \cdot \mathbf{t}_1 = 0$ and $\mathbf{t}_3 \cdot \mathbf{t}_1 = 0$. For example, if we choose $\mathbf{t}_1 = (1, i, -1)$ where $i^2 = -1$, then $\mathbf{t}_2 = (1/2, -i/2, 1)$ and $\mathbf{t}_3 = (i/2, -3/2, -i)$ satisfy the constraints on \mathbf{t}_i given above. Therefore, the following equation can be easily shown to be a solution of the diffusion equation (1):

$$\mathbf{j}^n(x, y, z) = \sinh(\sqrt{\mathbf{L}^n} (x + yi + z)) \left\{ \mathbf{A}'_0 + \frac{1}{2}(x - yi + 2z) \mathbf{A}'_1 + \frac{1}{2}(xi - 3y - 2i) \mathbf{A}'_2 \right. \\ \left. + \frac{1}{4}(x - yi + 2z)(xi - 3y - 2i) \mathbf{A}'_3 \right\}. \quad (4)$$

As in the original AFEN method, we choose nine \mathbf{t}_i 's so that they are evenly distributed 45 degrees apart on three unit circles on the x-y, y-z, and z-x planes, as follows:

$$(1,0,0), (0,1,0), (0,0,1), \left(\frac{\sqrt{2}}{2}, \frac{\sqrt{2}}{2}, 0 \right), \left(\frac{\sqrt{2}}{2}, -\frac{\sqrt{2}}{2}, 0 \right), \left(0, \frac{\sqrt{2}}{2}, \frac{\sqrt{2}}{2} \right), \left(0, \frac{\sqrt{2}}{2}, -\frac{\sqrt{2}}{2} \right), \left(\frac{\sqrt{2}}{2}, 0, \frac{\sqrt{2}}{2} \right), \left(-\frac{\sqrt{2}}{2}, 0, \frac{\sqrt{2}}{2} \right)$$

Noting that there are eight basis functions corresponding to each chosen \mathbf{t}_1 , we can include total 72 basis functions satisfying the diffusion equations in the flux expansion. However, as indicated in the introduction section, we have maximum 49 nodal unknowns including all neutron fluxes and flux moments to expand the intranodal flux distribution. Since one flux moment can be defined at each node-edge, it should be noted that only the flux moments weighted by the odd function of z are available for the intranodal flux expansion at the edges which become points when they are projected on the x-y plane. Therefore, for the fourth and the fifth \mathbf{t}_i 's in

Eq. (2) which correspond to these edges, we include only four basis functions, i.e., the sine and cosine hyperbolic functions of $\mathbf{t}_1 \cdot \mathbf{r}$, and their products multiplied by the linear function of z . Otherwise, we cannot succeed in expanding the intranodal flux distribution into the given nodal unknowns. Similarly, we include four basis functions for the last four \mathbf{t}_1 's in Eq. (2).

Now, the intranodal homogeneous flux in node n is expanded into 49 terms including a constant term;

$$\hat{\mathbf{f}}^n(x, y, z) = \mathbf{E} + \mathbf{j}^n(x, y, z) + \mathbf{j}^n(y, z, x) + \mathbf{j}^n(z, x, y), \quad (5)$$

where

$$\begin{aligned} \mathbf{j}^n(x, y, z) = & \sinh\left(\sqrt{\mathbf{L}^n x}\right)\{\mathbf{A}_0^x + y\mathbf{A}_1^x + z\mathbf{A}_2^x + yz\mathbf{A}_3^x\} + \cosh\left(\sqrt{\mathbf{L}^n x}\right)\{\mathbf{B}_0^x + y\mathbf{B}_1^x + z\mathbf{B}_2^x + yz\mathbf{B}_3^x\} \\ & + \sinh\left(\frac{\sqrt{2\mathbf{L}^n}}{2}(x+y)\right)\{\mathbf{C}_{00}^x + z\mathbf{D}_{00}^x\} + \cosh\left(\frac{\sqrt{2\mathbf{L}^n}}{2}(x+y)\right)\{\mathbf{C}_{01}^x + z\mathbf{D}_{01}^x\} \\ & + \sinh\left(\frac{\sqrt{2\mathbf{L}^n}}{2}(x-y)\right)\{\mathbf{C}_{10}^x + z\mathbf{D}_{10}^x\} + \cosh\left(\frac{\sqrt{2\mathbf{L}^n}}{2}(x-y)\right)\{\mathbf{C}_{11}^x + z\mathbf{D}_{11}^x\}. \end{aligned} \quad (6)$$

The reason why the constant term \mathbf{E} is introduced in the flux expansion and its function are described in Ref.[1]. Note that this constant term will vanish when k_{eff} converges during the iterative solution process.

The coefficients \mathbf{A}_i^u , \mathbf{B}_i^u , \mathbf{C}_{ij}^u , \mathbf{D}_{ij}^u , and \mathbf{E} in the flux expansion (6) are to be determined in terms of the nodal unknowns such as the node average flux, the interface fluxes, the interface moments, the edge fluxes, and the edge moments. For a three-dimensional node, it is very complicated to demonstrate the process to express all 49 coefficients into 49 nodal unknowns. Therefore, we explain here the process for a two-dimensional square node with side-length of h shown in Fig. 1. The equivalent flux expansion for the two-dimensional node is given by

$$\begin{aligned} \hat{\mathbf{f}}^n(x, y) = & \mathbf{E} + \sinh\left(\sqrt{\mathbf{L}^n x}\right)\{\mathbf{A}_0^x + y\mathbf{A}_1^x\} + \cosh\left(\sqrt{\mathbf{L}^n x}\right)\{\mathbf{B}_0^x + y\mathbf{B}_1^x\} \\ & + \sinh\left(\sqrt{\mathbf{L}^n y}\right)\{\mathbf{A}_0^y + x\mathbf{A}_1^y\} + \cosh\left(\sqrt{\mathbf{L}^n y}\right)\{\mathbf{B}_0^y + x\mathbf{B}_1^y\} \\ & + \sinh\left(\frac{\sqrt{2\mathbf{L}^n}}{2}(x+y)\right)\mathbf{C}_{00}^x + \cosh\left(\frac{\sqrt{2\mathbf{L}^n}}{2}(x+y)\right)\mathbf{C}_{01}^x \\ & + \sinh\left(\frac{\sqrt{2\mathbf{L}^n}}{2}(x-y)\right)\mathbf{C}_{10}^x + \cosh\left(\frac{\sqrt{2\mathbf{L}^n}}{2}(x-y)\right)\mathbf{C}_{11}^x. \end{aligned} \quad (7)$$

This expansion contains only 13 terms whose coefficients are expressed into 13 nodal unknowns comprising a node average flux, four interface fluxes, four interface moments, and four corner-point fluxes as shown in Fig. 1. Applying the coordinate system in the figure, the node average flux becomes

$$\begin{aligned} \bar{\mathbf{f}}^n = & \frac{1}{h^2} \int_{-\frac{h}{2}}^{\frac{h}{2}} \int_{-\frac{h}{2}}^{\frac{h}{2}} \hat{\mathbf{f}}^n(x, y) dy dx \\ = & \mathbf{E} + \left(\frac{\sqrt{\mathbf{L}^n h}}{2}\right)^{-1} \sinh\left(\frac{\sqrt{\mathbf{L}^n h}}{2}\right) (\mathbf{B}_0^x + \mathbf{B}_0^y) + \left(\frac{\sqrt{2\mathbf{L}^n h}}{4}\right)^{-2} \sinh^2\left(\frac{\sqrt{2\mathbf{L}^n h}}{4}\right) (\mathbf{C}_{01}^x + \mathbf{C}_{11}^x), \end{aligned} \quad (8)$$

where the bar (-) on a quantity indicates the average quantity over the node volume. The corner-point flux at point $(-h/2, -h/2)$ is given by

$$\begin{aligned}
\hat{\mathbf{f}}_{00}^x &= \hat{\mathbf{f}}^n \left(-\frac{h}{2}, -\frac{h}{2} \right) \\
&= \mathbf{E} - \sinh \left(\frac{\sqrt{\mathbf{L}^n h}}{2} \right) \left\{ \mathbf{A}_0^x + \mathbf{A}_0^y - \frac{h}{2} \mathbf{A}_1^x - \frac{h}{2} \mathbf{A}_1^y \right\} + \cosh \left(\frac{\sqrt{\mathbf{L}^n h}}{2} \right) \left\{ \mathbf{B}_0^x + \mathbf{B}_0^y - \frac{h}{2} \mathbf{B}_1^x - \frac{h}{2} \mathbf{B}_1^y \right\} \\
&\quad - \sinh \left(\frac{\sqrt{2\mathbf{L}^n h}}{2} \right) \mathbf{C}_{00}^x + \cosh \left(\frac{\sqrt{2\mathbf{L}^n h}}{2} \right) \mathbf{C}_{01}^x + \mathbf{C}_{11}^x.
\end{aligned} \tag{9}$$

The interface flux at interface $x=-h/2$ is given by

$$\begin{aligned}
\tilde{\mathbf{f}}_{x0}^n &= \frac{1}{h} \int_{-\frac{h}{2}}^{\frac{h}{2}} \hat{\mathbf{f}}^n \left(-\frac{h}{2}, y \right) dy \\
&= \mathbf{E} - \sinh \left(\frac{\sqrt{\mathbf{L}^n h}}{2} \right) \mathbf{A}_0^x + \cosh \left(\frac{\sqrt{\mathbf{L}^n h}}{2} \right) \mathbf{B}_0^x + \left(\frac{\sqrt{\mathbf{L}^n h}}{2} \right)^{-1} \sinh \left(\frac{\sqrt{\mathbf{L}^n h}}{2} \right) \left\{ \mathbf{B}_0^y - \frac{h}{2} \mathbf{B}_1^y \right\} \\
&\quad - \left(\frac{\sqrt{2\mathbf{L}^n h}}{4} \right)^{-1} \sinh \left(\frac{\sqrt{2\mathbf{L}^n h}}{4} \right) \left\{ \sinh \left(\frac{\sqrt{2\mathbf{L}^n h}}{4} \right) (\mathbf{C}_{00}^x + \mathbf{C}_{10}^x) - \cosh \left(\frac{\sqrt{2\mathbf{L}^n h}}{4} \right) (\mathbf{C}_{01}^x + \mathbf{C}_{11}^x) \right\}.
\end{aligned} \tag{10}$$

where the tilde (\sim) on a quantity indicates the average quantity over the interface.

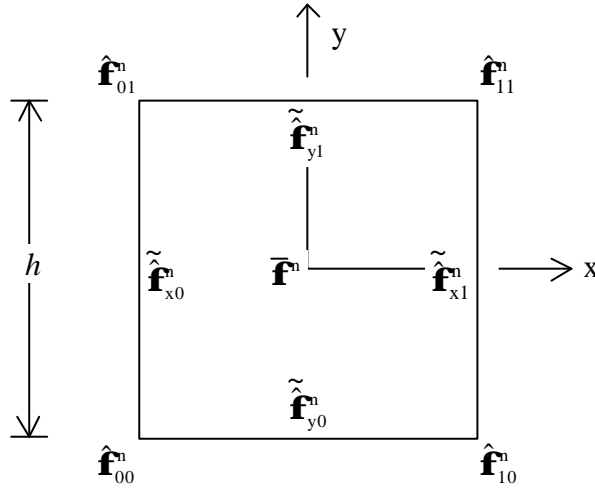


Fig. 1. Geometry of Node n

We obtained already nine equations to solve for the expansion coefficients, i.e., the equations (8) through (10) and their analogous expressions for three other interface fluxes and three other corner-point fluxes. Still, four more equations are needed to solve for the 13 expansion coefficients in the flux expansion (6). These equations can be obtained by introducing the interface flux moment defined as a weighted-average over the interface:

$$\tilde{\mathbf{y}}_{x0}^n = \frac{1}{h} \int_{-\frac{h}{2}}^{\frac{h}{2}} w(y) \hat{\mathbf{f}}^n \left(-\frac{h}{2}, y \right) dy, \tag{11}$$

where $w(y)$ is a weighting function given by an odd function of y . Physically, since the flux should be continuous at any point on an interface, this flux moment should also be continuous across the interface. Two types of $w(y)$, i.e., the step function and the linear function of y are examined as the weighting function in this paper:

$$w(y) = \begin{cases} -1 & \text{for } y < 0 \\ 1 & \text{for } y \geq 0 \end{cases} \quad \text{and} \quad w(y) = y. \tag{12}$$

It should be noted that the continuity of the flux and the flux moment with the step weighting function is completely equivalent to the flux continuity across each half of the interface. The current moment corresponding to the flux moment (11) is defined by

$$\tilde{\mathbf{j}}_{x0}^n = -\frac{\mathbf{D}^n}{h} \int_{-\frac{h}{2}}^{\frac{h}{2}} w(y) \frac{\partial}{\partial x} \hat{\mathbf{f}}^n(x, y) dy \Big|_{x=-\frac{h}{2}} \quad (13)$$

and must be continuous at the interface for the same reason.

For a three-dimensional node, three moments can be defined at interface $x=-h/2$ each of which corresponds to one of the three weighting functions $w(y)$, $w(z)$, and $w(y)w(z)$. Two types of weighting functions given by Eq. (12) are still choices for these moments. If we choose the step function as the weighting function, it is equivalent that we apply the flux and current continuity across each quadrant of an interface.

Our derivation will continue with the flux moment using the step weighting function. The flux moment (11) becomes,

$$\begin{aligned} \tilde{\mathbf{y}}_{x0}^n = & -\frac{h}{4} \sinh\left(\frac{\sqrt{\mathbf{L}^n h}}{2}\right) \mathbf{A}_1^x + \frac{h}{4} \cosh\left(\frac{\sqrt{\mathbf{L}^n h}}{2}\right) \mathbf{B}_1^x + \left(\frac{\sqrt{\mathbf{L}^n h}}{2}\right)^{-1} \left\{ \cosh\left(\frac{\sqrt{\mathbf{L}^n h}}{2}\right) - \mathbf{I} \right\} \left\{ \mathbf{A}_0^y - \frac{h}{2} \mathbf{A}_1^y \right\} \\ & + \left(\frac{\sqrt{2\mathbf{L}^n h}}{8}\right)^{-1} \sinh^2\left(\frac{\sqrt{2\mathbf{L}^n h}}{8}\right) \left\{ \cosh\left(\frac{\sqrt{2\mathbf{L}^n h}}{2}\right) (\mathbf{C}_{00}^x - \mathbf{C}_{10}^x) + \cosh\left(\frac{\sqrt{2\mathbf{L}^n h}}{2}\right) (\mathbf{C}_{01}^x - \mathbf{C}_{11}^x) \right\}, \end{aligned} \quad (14)$$

where \mathbf{I} is a unit matrix.

Including this equation and its analogous expressions for three other interface flux moments, we obtain the whole 13 equations to solve for all the 13 coefficients. All coefficients \mathbf{A}_i^u , \mathbf{B}_i^u , \mathbf{C}_{ij}^u , \mathbf{D}_{ij}^u , and \mathbf{E} are now expressed into the nodal unknowns such as the average flux, the interface fluxes, the interface moments, and the corner-point fluxes. For example, \mathbf{A}_2^x is given by

$$\begin{aligned} \mathbf{A}_2^x = & \left\{ \mathbf{I} - \left(\frac{\sqrt{\mathbf{L}^n h}}{2}\right)^{-1} \tanh\left(\frac{\sqrt{\mathbf{L}^n h}}{2}\right) \right\}^{-1} \left\{ \mathbf{I} - \left(\frac{\sqrt{2\mathbf{L}^n h}}{4}\right)^{-1} \tanh\left(\frac{\sqrt{2\mathbf{L}^n h}}{4}\right) \right\}^{-1} \cdot \\ & \left[\left(\frac{\sqrt{2\mathbf{L}^n h}}{4}\right)^{-1} \tanh\left(\frac{\sqrt{2\mathbf{L}^n h}}{4}\right) \frac{1}{4} \sum_{ij} \delta \hat{\mathbf{f}}_{ij}^n + \left\{ \mathbf{I} - \left(\frac{\sqrt{2\mathbf{L}^n h}}{4}\right)^{-1} \tanh\left(\frac{\sqrt{2\mathbf{L}^n h}}{4}\right) \right\} \frac{1}{2} \left\{ \tilde{\mathbf{f}}_{x0}^n + \tilde{\mathbf{f}}_{x1}^n - \bar{\mathbf{f}}^n \right\} \right], \end{aligned} \quad (15)$$

where the indices i and j run over all points, and

$$\delta \hat{\mathbf{f}}_{ij}^n = \hat{\mathbf{f}}_{ij}^n - \tilde{\mathbf{f}}_{xi}^n - \tilde{\mathbf{f}}_{yj}^n + \bar{\mathbf{f}}^n. \quad (16)$$

II.B. Nodal Coupling Equations

The nodal unknowns in the homogeneous flux expansions in a node are inter-coupled to the unknowns for neighboring nodes through the nodal coupling equations. Such coupling equations are composed of the ones to be solved for each type of the nodal unknowns. Since we use the node average fluxes, the interface fluxes, the interface moments, and the corner-point fluxes as unknowns, we need four types of nodal coupling equations that correspond to each of them.

For the convenience of deriving nodal coupling equations, we first express the interface

current, the interface current moment, and the corner-point leakage into nodal unknowns. Differentiating the intranodal flux, we can obtain the expression for the interface current \mathbf{J}_{x1} shown in Fig. 1 in terms of the nodal unknowns:

$$\begin{aligned}\tilde{\mathbf{J}}_{x0}^n &= -\frac{\mathbf{D}^n}{h} \int_{-\frac{h}{2}}^{\frac{h}{2}} \frac{\partial \hat{\mathbf{f}}^n(x, y)}{\partial x} dy \Big|_{x=-\frac{h}{2}} \\ &= \mathbf{T}_{J1}^n \frac{1}{2} \left(\tilde{\mathbf{f}}_{x0}^n + \tilde{\mathbf{f}}_{x1}^n \right) + \mathbf{T}_{J2}^n \frac{1}{2} \left(\tilde{\mathbf{f}}_{x0}^n - \tilde{\mathbf{f}}_{x1}^n \right) + \mathbf{T}_{J3}^n \frac{1}{4} \left(\delta \hat{\mathbf{f}}_{00}^n + \delta \hat{\mathbf{f}}_{01}^n + \delta \hat{\mathbf{f}}_{10}^n + \delta \hat{\mathbf{f}}_{11}^n \right) \\ &\quad + \mathbf{T}_{J4}^n \frac{1}{4} \left(\delta \hat{\mathbf{f}}_{00}^n + \delta \hat{\mathbf{f}}_{01}^n - \delta \hat{\mathbf{f}}_{10}^n - \delta \hat{\mathbf{f}}_{11}^n \right) + \mathbf{T}_{J5}^n \frac{1}{2} \left(\tilde{\mathbf{y}}_{y0}^n + \tilde{\mathbf{y}}_{y1}^n \right) - \mathbf{T}_{J1}^n \bar{\mathbf{f}}^n,\end{aligned}\quad (17)$$

where

$$\mathbf{T}_{J1}^n = \frac{8}{h} \mathbf{D}^n \left\{ \mathbf{r}_1^n \left(\mathbf{r}_1^n - \mathbf{t}_1^n \right) \right\}^{-1} \left(\mathbf{t}_1^n - \mathbf{I} \right), \quad (18)$$

$$\mathbf{r}_1^n = \left(\frac{\sqrt{\mathbf{L}^n h}}{4} \right)^{-1} \tanh \left(\frac{\sqrt{\mathbf{L}^n h}}{4} \right), \quad (19)$$

$$\mathbf{t}_1^n = \frac{1}{16} \left(\mathbf{r}_1^n \right)^2 \mathbf{L}^n h^2 + \mathbf{I}, \quad (20)$$

and the other \mathbf{T}_{ji}^n 's are given similarly.

Differentiating the flux moment at the interface gives the expression for the interface current moment:

$$\begin{aligned}\tilde{\mathbf{j}}_{x0}^n &= -\frac{\mathbf{D}^n}{h} \int_{-\frac{h}{2}}^{\frac{h}{2}} w(y) \frac{\partial \hat{\mathbf{f}}^n(x, y)}{\partial x} dy \Big|_{x=-\frac{h}{2}} \\ &= \mathbf{T}_{j1}^n \frac{1}{2} \left(\tilde{\mathbf{y}}_{x0}^n + \tilde{\mathbf{y}}_{x1}^n \right) + \mathbf{T}_{j2}^n \frac{1}{2} \left(\tilde{\mathbf{y}}_{x0}^n - \tilde{\mathbf{y}}_{x1}^n \right) + \mathbf{T}_{j3}^n \frac{1}{2} \left(\tilde{\mathbf{y}}_{y0}^n - \tilde{\mathbf{y}}_{y1}^n \right) + \mathbf{T}_{j4}^n \frac{1}{2} \left(\tilde{\mathbf{f}}_{y0}^n - \tilde{\mathbf{f}}_{y1}^n \right) \\ &\quad + \mathbf{T}_{j5}^n \frac{1}{4} \left(\delta \hat{\mathbf{f}}_{01}^n - \delta \hat{\mathbf{f}}_{00}^n + \delta \hat{\mathbf{f}}_{11}^n - \delta \hat{\mathbf{f}}_{10}^n \right) + \mathbf{T}_{j6}^n \frac{1}{4} \left(\delta \hat{\mathbf{f}}_{01}^n - \delta \hat{\mathbf{f}}_{00}^n - \delta \hat{\mathbf{f}}_{11}^n + \delta \hat{\mathbf{f}}_{10}^n \right),\end{aligned}\quad (21)$$

where \mathbf{T}_{ji}^n 's are matrix functions of the cross-section matrix as indicated in Eq. (18).

The corner-point leakage that is defined as the sum of two differences of local directional currents at a corner point and the currents at the interfaces sharing the corner point is expressed in the following form:

$$\begin{aligned}\mathbf{L}_{00}^n &= -\frac{\mathbf{D}^n}{h} \left(\frac{\partial \hat{\mathbf{f}}^n(x, y)}{\partial x} + \frac{\partial \hat{\mathbf{f}}^n(x, y)}{\partial y} \right) \Big|_{x=-\frac{h}{2}}^{y=-\frac{h}{2}} - \left(\tilde{\mathbf{J}}_{x0}^n + \tilde{\mathbf{J}}_{y0}^n \right) \\ &= \mathbf{T}_{L1}^n \frac{1}{4} \left(\delta \hat{\mathbf{f}}_{00}^n + \delta \hat{\mathbf{f}}_{01}^n + \delta \hat{\mathbf{f}}_{10}^n + \delta \hat{\mathbf{f}}_{11}^n \right) + \mathbf{T}_{L2}^n \frac{1}{2} \left(\delta \hat{\mathbf{f}}_{00}^n - \delta \hat{\mathbf{f}}_{11}^n \right) \\ &\quad + \mathbf{T}_{L3}^n \frac{1}{4} \left(\delta \hat{\mathbf{f}}_{00}^n - \delta \hat{\mathbf{f}}_{01}^n - \delta \hat{\mathbf{f}}_{10}^n + \delta \hat{\mathbf{f}}_{11}^n \right) + \mathbf{T}_{L4}^n \frac{1}{2} \left(\tilde{\mathbf{f}}_{x0}^n + \tilde{\mathbf{f}}_{y0}^n - \tilde{\mathbf{f}}_{x1}^n - \tilde{\mathbf{f}}_{y1}^n \right) \\ &\quad + \mathbf{T}_{L5}^n \frac{1}{2} \left(\tilde{\mathbf{y}}_{x0}^n + \tilde{\mathbf{y}}_{y0}^n + \tilde{\mathbf{y}}_{x1}^n + \tilde{\mathbf{y}}_{y1}^n \right) + \mathbf{T}_{L6}^n \frac{1}{2} \left(\tilde{\mathbf{y}}_{x0}^n + \tilde{\mathbf{y}}_{y0}^n - \tilde{\mathbf{y}}_{x1}^n - \tilde{\mathbf{y}}_{y1}^n \right),\end{aligned}\quad (22)$$

where \mathbf{T}_{Li}^n 's are also matrix functions of the cross-section matrix.

The first type of nodal coupling equations to be solved for the node average fluxes is derived by considering the neutron balance of a node:

$$\frac{1}{h} \left(\tilde{\mathbf{J}}_{i+1j}^x - \tilde{\mathbf{J}}_{ij}^x \right) + \frac{1}{h} \left(\tilde{\mathbf{J}}_{ij+1}^y - \tilde{\mathbf{J}}_{ij}^y \right) + \mathbf{S}^{ij} \bar{\mathbf{f}}_{ij} = \frac{1}{k_{\text{eff}}} \nu \mathbf{S}_f^{ij} \bar{\mathbf{f}}_{ij}. \quad (23)$$

Then, with substitution of the interface current (17), this equation becomes

$$\left\{ \mathbf{S}^{ij} + \frac{4}{h} (\mathbf{T}_{J1}^{ij} - \mathbf{T}_{J3}^{ij}) \right\} \bar{\mathbf{f}}_{ij} = \frac{1}{k_{\text{eff}}} \mathbf{v} \mathbf{S}_f^{ij} \bar{\mathbf{f}}_{ij} + \frac{1}{h} (\mathbf{T}_{J1}^{ij} - 2\mathbf{T}_{J3}^{ij}) (\tilde{\mathbf{F}}^{ij})^{-1} (\tilde{\mathbf{f}}_{ij}^x + \tilde{\mathbf{f}}_{i+1j}^x + \tilde{\mathbf{f}}_{ij}^y + \tilde{\mathbf{f}}_{ij+1}^y) + \frac{1}{h} \mathbf{T}_{J3}^n (\mathbf{F}^{ij})^{-1} (\mathbf{f}_{ij} + \mathbf{f}_{i+1j} + \mathbf{f}_{ij+1} + \mathbf{f}_{i+1j+1}) + \frac{1}{h} \mathbf{T}_{J5}^n (\tilde{\mathbf{F}}^{ij})^{-1} (\tilde{\mathbf{y}}_{ij}^x + \tilde{\mathbf{y}}_{i+1j}^x + \tilde{\mathbf{y}}_{ij}^y + \tilde{\mathbf{y}}_{ij+1}^y), \quad (24)$$

where $\tilde{\mathbf{F}}^{ij}$ and \mathbf{F}^{ij} are the interface discontinuity factor and the corner-point discontinuity factor, respectively. The homogeneous fluxes and moments in the interface current equation (17) are transformed into the heterogeneous ones according to the equivalence theory. [4,5] It is assumed that a single interface discontinuity factor and a single corner-point discontinuity factor are available for all the interfaces and the corner points of the node, respectively, and that the interface discontinuity factor is also effective for the interface flux moments. This seems inevitable when we calculate the discontinuity factors by a single-assembly homogenization with the zero-current boundary condition for a symmetric assembly. The discontinuity factor for the interface flux moment can be defined in a consistent way to the definition of the flux moment in the case of a multiassembly homogenization, or a single-assembly homogenization with non-zero boundary condition, or a homogenization for an asymmetric assembly. The use of the consistent discontinuity factor for the interface flux moment may mitigate the difficulties in homogenizing fuel assemblies with geometrical or material complexities.

The second type of coupling equations which can be solved for the interface fluxes is derived by the continuity condition of the neutron current across the interface between nodes $i-1j$ and ij in Fig.2:

$$\begin{aligned} & \frac{1}{2} \sum_{k=0,1} (\mathbf{T}_{J1}^{i-kj} - \mathbf{T}_{J2}^{i-kj} - \mathbf{T}_{J3}^{i-kj} + \mathbf{T}_{J4}^{i-kj}) (\tilde{\mathbf{F}}^{i-kj})^{-1} \tilde{\mathbf{f}}_{i-2k+1j}^x + \frac{1}{2} \sum_{k=0,1} (\mathbf{T}_{J1}^{i-kj} + \mathbf{T}_{J2}^{i-kj} - \mathbf{T}_{J3}^{i-kj} - \mathbf{T}_{J4}^{i-kj}) (\tilde{\mathbf{F}}^{i-kj})^{-1} \tilde{\mathbf{f}}_{ij}^x \\ &= -\frac{1}{4} \sum_{k=0,1} (\mathbf{T}_{J3}^{i-kj} - \mathbf{T}_{J4}^{i-kj}) (\mathbf{F}^{i-kj})^{-1} (\mathbf{f}_{i-2k+1j+1} + \mathbf{f}_{i-2k+1j}) - \frac{1}{4} \sum_{k=0,1} (\mathbf{T}_{J3}^{i-kj} + \mathbf{T}_{J4}^{i-kj}) (\mathbf{F}^{i-kj})^{-1} (\mathbf{f}_{ij+1} + \mathbf{f}_{ij}) \\ & - \frac{1}{2} \sum_{k=0,1} \mathbf{T}_{J5}^{i-kj} (\tilde{\mathbf{F}}^{i-kj})^{-1} (\tilde{\mathbf{y}}_{i-kj+1}^y + \tilde{\mathbf{y}}_{i-kj}^y) + \sum_{k=0,1} \mathbf{T}_{J1}^{i-kj} \bar{\mathbf{f}}_{i-kj}^{\bar{0}}. \end{aligned} \quad (25)$$

This equation is a block tridiagonal matrix equation, which is easily solved for $\tilde{\mathbf{f}}_{ij}^x$.

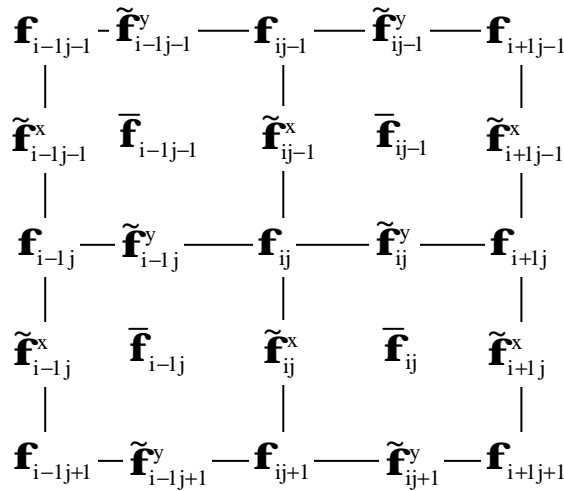


Fig. 2. Geometry for the Derivation of Nodal Coupling Equations

The continuity condition of the current moment across the interface yields the third type of

coupling equations solved for the flux moments:

$$\begin{aligned}
& \frac{1}{2} \sum_{k=0,1} (\mathbf{T}_{j1}^{i-kj} - \mathbf{T}_{j2}^{i-kj}) (\tilde{\mathbf{F}}^{i-kj})^{-1} \tilde{\mathbf{y}}_{i-2k+1j}^x + \frac{1}{2} \sum_{k=0,1} (\mathbf{T}_{j1}^{i-kj} + \mathbf{T}_{j2}^{i-kj}) (\tilde{\mathbf{F}}^{i-kj})^{-1} \tilde{\mathbf{y}}_{ij}^x \\
&= -\frac{1}{2} \sum_{k=0,1} \mathbf{T}_{j3}^{i-kj} (\tilde{\mathbf{F}}^{i-kj})^{-1} (\tilde{\mathbf{y}}_{i-kj+1}^y - \tilde{\mathbf{y}}_{i-kj}^y) - \frac{1}{2} \sum_{k=0,1} (\mathbf{T}_{j4}^{i-kj} + \mathbf{T}_{j5}^{i-kj}) (\tilde{\mathbf{F}}^{i-kj})^{-1} (\tilde{\mathbf{f}}_{i-kj+1}^y - \tilde{\mathbf{f}}_{i-kj}^y) \\
& - \frac{1}{4} \sum_{k=0,1} (\mathbf{T}_{j5}^{i-kj} - \mathbf{T}_{j6}^{i-kj}) (\mathbf{F}^{i-kj})^{-1} (\mathbf{f}_{i-2k+1j+1} - \mathbf{f}_{i-2k+1j}) - \frac{1}{4} \sum_{k=0,1} (\mathbf{T}_{j5}^{i-kj} - \mathbf{T}_{j6}^{i-kj}) (\mathbf{F}^{i-kj})^{-1} (\mathbf{f}_{ij+1} - \mathbf{f}_{ij}).
\end{aligned} \tag{26}$$

This is a block tridiagonal matrix equation for the flux moment $\tilde{\mathbf{y}}_{ij}^x$.

Finally, the coupling equations for the corner-point fluxes are obtained by considering the leakage balance around the corner point ij shared by nodes ij , $i-1j$, $ij-1$, and $i-1j-1$:

$$\begin{aligned}
& \frac{1}{4} \sum_{\substack{u=0,1 \\ v=0,1}} (\mathbf{T}_{L1}^{i-uj-v} + 2\mathbf{T}_{L2}^{i-uj-v} + \mathbf{T}_{L3}^{i-uj-v}) (\mathbf{F}^{i-uj-v})^{-1} \mathbf{f}_{ij} \\
& + \frac{1}{4} \sum_{\substack{u=0,1 \\ v=0,1}} (\mathbf{T}_{L1}^{i-uj-v} - \mathbf{T}_{L3}^{i-uj-v}) (\mathbf{F}^{i-uj-v})^{-1} (\mathbf{f}_{i-2u+1j} + \mathbf{f}_{ij-2v+1}) \\
& + \frac{1}{4} \sum_{\substack{u=0,1 \\ v=0,1}} (\mathbf{T}_{L1}^{i-uj-v} - 2\mathbf{T}_{L2}^{i-uj-v} + \mathbf{T}_{L3}^{i-uj-v}) (\mathbf{F}^{i-uj-v})^{-1} \mathbf{f}_{i-2u+1j-2v+1} \\
&= -\frac{1}{2} \sum_{\substack{u=0,1 \\ v=0,1}} (\mathbf{T}_{L4}^{i-uj-v} - \mathbf{T}_{L1}^{i-uj-v} - \mathbf{T}_{L2}^{i-uj-v}) (\tilde{\mathbf{F}}^{i-uj-v})^{-1} (\tilde{\mathbf{f}}_{ij-v}^x + \tilde{\mathbf{f}}_{i-uj}^y) \\
& - \frac{1}{2} \sum_{\substack{u=0,1 \\ v=0,1}} (\mathbf{T}_{L4}^{i-uj-v} - \mathbf{T}_{L1}^{i-uj-v} + \mathbf{T}_{L2}^{i-uj-v}) (\tilde{\mathbf{F}}^{i-uj-v})^{-1} (\tilde{\mathbf{f}}_{i-2u+1j-v}^x + \tilde{\mathbf{f}}_{i-uj-2v+1}^y) \\
& - \frac{1}{2} \sum_{\substack{u=0,1 \\ v=0,1}} (\mathbf{T}_{L5}^{i-uj-v} + \mathbf{T}_{L6}^{i-uj-v}) (\tilde{\mathbf{F}}^{i-uj-v})^{-1} (\tilde{\mathbf{y}}_{ij-v}^x + \tilde{\mathbf{y}}_{i-uj}^y) \\
& - \frac{1}{2} \sum_{\substack{u=0,1 \\ v=0,1}} (\mathbf{T}_{L5}^{i-uj-v} - \mathbf{T}_{L6}^{i-uj-v}) (\tilde{\mathbf{F}}^{i-uj-v})^{-1} (\tilde{\mathbf{y}}_{i-2u+1j-v}^x + \tilde{\mathbf{y}}_{i-uj-2v+1}^y).
\end{aligned} \tag{27}$$

This equation is a nine-point equation for $\tilde{\mathbf{y}}_{ij}^x$. In spite of its complicated structure, it is usually easily solved by the conventional iterative techniques.

The four types of nodal coupling equations, (24) through (27) are now available for an iteration procedure. The conventional scheme consisting of two levels of iterations, i.e., inner iteration and outer iteration may be used.

III. Numerical Results and Discussion

Choosing benchmark problems to test the refined AFEN method developed here is very careful, because the original AFEN method against which the refined method should show its accuracy improvement is so accurate for most problems. The problems with the explicit baffle and reflector model are not adequate for this purpose because its accuracy improvement could be hidden behind the relatively large errors caused by the baffle/reflector homogenization. Choosing the problems with smooth flux distribution does not seem good either to show the relative superiority of such a sophisticated method as the AFEN method.

The C5 configuration of the OECD-L336 problem[7] does not have a baffle region and

bears the great flux change over its small core volume. The great flux change is seen in the region near the interface between the uranium-oxide fuel assembly and the mixed-oxide fuel assembly and the interface between fuel and reflector.

The fuel assemblies have different types of 17x17 pin-cells and were homogenized by the single-assembly calculations with the zero current boundary condition. The AFEN calculations with node size of a pin-cell thickness (1.26cm) were used for both the homogenization calculations and the reference flux calculation of the problem, because the AFEN calculation with such a small node size can exclude almost all the discretization errors and can achieve the required accuracy in comparison of the AFEN method and the refined AFEN method.

In Fig. 3a, the nodal unknowns and the effective multiplication factor calculated by three nodal methods were compared with those of the fine mesh AFEN calculation. The first calculation was performed by the original AFEN method. The second one was by the method that uses the interface flux moments as nodal unknowns instead of the corner-point fluxes in the original AFEN method. The third method uses both the interface flux moments and the corner-point fluxes as unknowns. The step weighting function is used to define the flux moment for the last two calculations, because we could not see any significant difference between the results using the step weighting function and the linear weighting function. As expected from the fact that the number of conditions constraining the intranodal flux distribution is unchanged, it cannot be easily judged which one is better between the original AFEN method and the second method using the interface moments only. This shows that there is no accuracy degradation in substituting the corner-point fluxes with the interface moments in the unknown system of the AFEN method. In spite of the accuracy improvement in the core peripheral nodes including reflector nodes, one cannot clearly see the superiority of the refined AFEN method taking both the corner-point fluxes and the interface moments as unknowns. This is because the main error source is still the model deficiency in homogenization of the heterogeneous fuel assemblies. To exclude the homogenization error completely, we performed the fine-mesh AFEN reference calculation after replacing all the fuel assemblies by the equivalently homogenized fuels, and repeated the comparison among the three methods in Fig. 3b. The error reduction in the effective multiplication factor and the flux distribution by the refined AFEN method is more clearly shown in this figure.

Since there is not much need to improve the accuracy of the original AFEN method, the other salient features of the refined AFEN method would rather be important than its accuracy improvement, as indicated in the introduction section. The method that replaces the corner-point fluxes with the interface flux moments can easily be adopted into the existing nodal codes with interface nodal unknowns only and may fit better for the non-linear iterative scheme based on two-node problems.

IV. Conclusions

A refinement of the AFEN method has been performed by increasing the number of flux expansion terms in the manner that the original expansion basis functions are combined with the transverse-direction linear functions. In this manner, the added terms can be kept to still satisfy the diffusion equation at any point in the node. The flux moments introduced at the interfaces provide the constraints required additionally by these added terms. The interface flux moments are defined by the average values of the fluxes weighted by odd functions in the

parallel directions to the interface. Two choices of the weighting functions, i.e., a step or a linear function are examined here. Since the refined flux expansion also satisfies the diffusion equation and the additional constraints are applied, the salient feature of the original AFEN method is even more enforced in the refined method.

The refined AFEN method was tested against a mixed-oxide fuel benchmark problem in two-dimensional rectangular geometry. The results show that the method improves the accuracy in predicting the homogeneous flux distribution and the effective multiplication factor.

Since the original AFEN method is accurate enough for most applications, the other salient features of the refined AFEN method would rather be important than the accuracy improvement of the refined method. Maintaining the accuracy, this method can replace the corner-point fluxes with the interface moments so that the method may be easily implemented into the existing nodal codes that do not use the corner-point fluxes as unknowns. It may fit better for the non-linear scheme based on two-node problems that are solved for the interface quantities of the two nodes and is expected better performance.

The extensions of the refined AFEN method to the hexagonal geometry and the three-dimensional geometry, the development of the non-linear iterative scheme that fits for this method, and the fidelity test of this method in reconstructing pin-fluxes are currently in progress.

References

1. Jae Man Noh and Nam Zin Cho, "A New Approach of Analytic Basis Function Expansion to Neutron Diffusion Nodal Calculation," *Nucl. Sci. Eng.*, **116**, 165 (1994).
2. Nam Zin Cho and Jae Man Noh, "Analytic Function Expansion Nodal Method for Hexagonal Geometry," *Nucl. Sci. Eng.*, **121**, 245 (1995).
3. Nam Zin Cho, Yong Hee Kim, and Keon Woo Park, "Extension of Analytic Function Expansion Nodal Method to Multigroup Problems in Hexagonal-Z Geometry," *Nucl. Sci. Eng.*, **126**, 35 (1997).
4. K. Koebke, "A New Approach to Homogenization and Group Condensation," *Proc. IAEA Technical Committee Mtg.*, Lugano, Switzerland, November 1978, IAEA-TECDOC 231, p.303, International Atomic Energy Agency (1978).
5. K. S. Smith, "Spatial Homogenization Methods for Light Water Reactor Analysis," PhD Thesis, Massachusetts Institute of Technology (1980).
6. Jae Man Noh, Leonid Pogobekyan, Young Jin Kim and Hyung Kook Joo, "A General Approach to Multigroup Extension of the Analytic Function Expansion Nodal Method Based on Matrix Function Theory," *Proc. 1996 Joint Intl. Conf. Mathematical Methods and Super Computing for Nuclear Applications*, Saratoga Springs, New York, October 6-10, 1997, Vol. **1**, p. 144, American Nuclear Society (1997).
7. J. C. Lefebvre, J. Mondot, and J. P. West, "Benchmark Calculations of Power Distribution within Assemblies," NEACRP-L-336, Organization for Economic Cooperation and Development (1991).

